PERGAMON

International Journal of Solids and Structures 40 (2003) 465–491

INTERNATIONAL JOURNAL OF SOLIDS and STRUCTURES

www.elsevier.com/locate/ijsolstr

Vibration suppression for high-speed railway bridges using tuned mass dampers

J.F. Wang [a], C.C. Lin [a,*], B.L. Chen [b]

[a] *Department of Civil Engineering, National Chung-Hsing University, Taichung, Taiwan, 402 ROC*
[b] *Department of Civil Engineering, National Lien-Ho Institute of Technology, Miaoli, Taiwan, 360 ROC*

Received 3 July 2001; received in revised form 4 October 2002

Abstract

This paper deals with the applicability of passive tuned mass dampers (PTMDs) to suppress train-induced vibration on bridges. A railway bridge is modeled as an Euler–Bernouli beam and a train is simulated as series of moving forces, moving masses or moving suspension masses to investigate the influence of various vehicle models on the bridge features with or without PTMD. According to the train load frequency analysis, the resonant effects will occur as the modal frequencies of the bridges are close to the multiple of the impact frequency of the train load to the bridge. A single PTMD system is then designed to alter the bridge dynamic characteristics to avoid excessive vibrations. Numerical results from simply supported bridges of Taiwan High-Speed Railway (THSR) under German I.C.E., Japanese S.K.S. and French T.G.V. trains show that the proposed PTMD is a useful vibration control device in reducing bridge vertical displacements, absolute accelerations, end rotations and train accelerations during resonant speeds, as the train axle arrangement is regular. It is also found that the inner space of bridge box girder of THSR is wide and deep enough for the installation and movement of PTMD.

Keywords: High-speed railway bridge; Tuned mass dampers; Train loads; Resonant train speed; Vibration suppression

1. Introduction

In general, transportation infrastructure is an important factor affecting the development of a national economy. Because of space and terrain limitations, more transportation structures, such as highways and railways, have been constructed as bridges in urban areas. With the rapid advances in the field of high performance materials and construction techniques, these bridges have a trend towards long and flexible as those of the high-rise buildings. When excessive external loads occur, these bridges may suffer large deflections and even cause damages that will endanger human life and property. In order to understand the dynamic behavior of bridges under natural loads such as wind or earthquake excitations, considerable

* Corresponding author. Tel./fax: +886-4-22851992.
E-mail addresses: jerfu@ms16.hinet.net (J.F. Wang), cclin3@dragon.nchu.edu.tw (C.C. Lin), blchen@mail.nlhu.edu.tw (B.L. Chen).

0020-7683/02/$ - see front matter
PII: S0020-7683(02)00589-9

Nomenclature

$A(x)$	bridge section area
$\mathbf{C}_\mathrm{b}$	bridge modal damping matrix
c_{b_j}	jth modal damping ratio of bridge
c_s	PTMD damping cofficient
$C_y(x)$	damping coefficient of bridge at section x
d	spacing of train loads
E	Young's modulus
$\mathbf{F}_\mathrm{b}$	modal train load vector
F_{b_j}	jth modal train load
g	gravity acceleration
$H_{\eta_j F}(\omega)$	transfer function of the jth modal dislpacement of bridge
$H_{v_s F}(\omega)$	transfer function of PTMD stroke
$I(x)$	moment of inertia of the bridge
$\mathbf{K}_\mathrm{b}$	bridge modal stiffness matrix
k_{b_j}	jth bridge modal stiffness coefficient
k_s	PTMD's stiffness coefficient
L	span length of the bridge
$\mathbf{M}_\mathrm{b}$	bridge modal mass matrix
$\bar{m}(x)$	bridge mass per unit length at section x
m_{b_j}	jth modal mass of bridge
m_s	PTMD mass
m_{v_k}	mass of the kth train load in the moving suspension mass model
N	number of mode to be considered
N_v	number of train load
p_k	magnitude of the kth train load in the moving force model
$P_\mathrm{b}(x,t)$	distributed force applied on the beam
R_{dv_j}	jth bridge modal response ratio
r_{f_j}	frequency ratio of PTMD to the controlled bridge mode
$U(-)$	unit step function
t	instantaneous time
t_k	time of the kth train load reaching the bridge
v	train speed
v_c	resonant train speed
v_s	PTMD stroke
x_s	position of PTMD on the bridge in the longitudinal direction
x	longitudinal position measured from supports of bridge
$y(x,t)$	bridge vertical displacement
$z_s(t)$	PTMD vertical displacement
$z_v(t)$	vertical displacement of the kth train load
$\delta(-)$	Dirac delta function
$\eta_j(t)$	jth modal displacement of bridge
$\boldsymbol{\eta}(t)$	modal displacement vector of bridge
μ_{s_j}	PTMD mass ratio
ξ_j	jth modal damping ratio of bridge

ξ_s	PTMD damping ratio
ω_j	jth modal frequency of bridge
ω_s	PTMD natural frequency
$\phi_j(x)$	jth mode-shape function of bridge
$\mathbf{\Phi}(x)$	mode-shape function matrix of bridge
$\mathbf{\Gamma}$	modal participation factor of the bridge-PTMD system

numerical and experimental efforts have been made over the past two decades (Abdel-Ghaffar and Rubin, 1982; Dumanoglu and Severn, 1990; Boonyapinyo et al., 1994).

The vibration of a bridge structure due to the passage of vehicles is also an important consideration in bridge design. To comprehend the complex interactions between the vehicle and the bridge and to develop rational design procedures, a number of analytical and experimental investigations have been carried out over the past few decades. In those studies, one of the main subjects was the simulation of vehicle systems. Traditionally, the vehicle was modeled as a moving force that assumed constant vehicular load in the bridge at any location (Vellozzi, 1967; Hayashikawa and Watanabe, 1981, 1982; Bryja and Sniady, 1988). Then, more accurate models, such as moving mass (Wilson and Barbas, 1980; Inbanathan and Wieland, 1987; Akin and Mofid, 1989), moving suspension mass (Humar and Kashif, 1995) and complicated two-dimensional (Veletsos and Huang, 1970; Hutton and Cheung, 1979; Huang and Wang, 1992; Green et al., 1995) or three-dimensional (Wang et al., 1992; Chatterjee et al., 1994; Kou and De Wolf, 1997; Huang and Wang, 1998; Huang et al., 1998) vehicle bodies, were developed to respectively take the inertial force, the suspension system, and the complex dynamic mechanisms of vehicles into account. Most of the previous researches involved highway bridges, where single vehicle or random moving vehicles were used as the external forces. Investigations involving the dynamic behavior of bridges under periodic moving loads which represent the impact of a train are relatively few (Klasztorny and Langer, 1990; Frýba, 1996), especially for the dynamics of railway bridges under high-speed trains. Chen and Li (2000) calculated the dynamic responses of THSR elevated railway bridges subjected to the French T.G.V., the German I.C.E., and the Japanese S.K.S. train loads with the maximum operation speed of 350 km/h. The bridge is constructed as a single-span or three-equal-span box girder supported on piers. Yang et al. (1997) obtained the conditions of resonance and cancellation for a simple beam due to train loads and proposed the optimal span length for bridges for a specified spacing of train loads. They found that if the optimal span length was not used, the bridge would undergo resonant effects because of the periodic arrangement of passenger cars as the train traveled at certain speeds. Frýba (2001) derived analytical formulas to obtain the resonant train speeds which appear actually on high-speed lines at today's train speed. Generally, these resonance conditions will result in large responses and are not expected for bridges. They will seriously affect train safety operations, the comfort of passengers, the service life of bridges and the utilization of the surrounding land, and even endanger the safety of supporting structures. Therefore, it is essential to find an appropriate way to reduce the excessive vibration of such bridges under train loads.

In the field of structural engineering, vibration control systems have been applied to reduce the dynamic responses of structures since the 1980s. One of the techniques used is the active/passive tuned mass damper (ATMD/PTMD), which can be incorporated into an existing structure with less interference as compared with other control devices. So far, this device has been installed in over 300 high-rise buildings against wind and earthquakes in the world. The corresponding theoretical and experimental investigations for this technique are still under continuous development. Most of the previous researches about PTMD systems are concerned with the mitigation of building vibrations. Only a few researchers have investigated the practical applications of PTMD in reducing the dynamic vibrations of bridges due to moving vehicles. Kajikawa et al. (1989) utilized a single PTMD on highway bridges and concluded that this passive control

device could not completely suppress traffic-induced vibrations since the dynamic responses of a bridge are frequency-variant due to vehicle motion. Kwon et al. (1998) inspected the PTMD control effectiveness on a high-speed railway continuous bridge with three spans in Korea. In their paper, a single PTMD with the parameters proposed by Den Hartog (1956) was used. The numerical results for the bridge subjected to the French T.G.V. train with a arbitrary train speed of 300 km/h showed that the PTMD with mass ratio of 1% was able to reduce the bridge vertical free displacement response for about 21% but less effective in suppressing the vertical acceleration of the passenger car because the vehicle passage time on the bridge is too short.

Presently, the planning and construction of a high-speed railway are the most important infrastructure project in Taiwan. The total length of the route is about 345 km. In order to save land value and construction time, most of the route will be constructed as a series of bridges. For THSR bridges, four dynamic response limitations for the bridges and the trains must be satisfied: (1) the vertical displacement of the bridge, (2) the vertical acceleration of the bridge, (3) the end rotation of the bridge, and (4) the vertical acceleration of the train. The objective of this paper is to investigate the PTMD vibration control effectiveness for the simply supported bridges proposed in the original THSR design proposal subjected to the German I.C.E., French T.G.V., and Japanese S.K.S. train loads. An optimal single PTMD, which is a single-degree-of-freedom (s.d.o.f.) system with mass, damping, and stiffness, was developed to reduce the above four dynamic responses. Further, not only the dynamic behavior characteristics of the bridges under high-speed train loads but also the PTMD detuning effect resulting from the interaction between the bridge and train are extensively examined in the following sections.

2. Bridge-PTMD systems under train loads

2.1. Modeling of bridge and train

In comparison with buildings subjected to wind or earthquake excitations, the location of train loads on bridges is time–variant. Further, because of the interaction effect between the train and bridge, the magnitude of the train load is dependent upon the response of the bridge. Therefore, it would be difficult to establish a clear correlation between the governing parameters and bridge responses if precise train models were used in the analytical studies. To clearly identify the dominant parameters and to obtain the analytical solutions, simplified models were usually employed in many researches (Vellozzi, 1967; Hayashikawa and Watanabe, 1981, 1982; Bryja and Sniady, 1988). Once the basic parameters have been identified, it is possible to refine the model to include other variables for advanced work. In this study, several assumptions were made to make the problem easier, as follows: (1) The bridge is regarded as a straight beam made of homogeneous, elastic, isotropic material. The supports of the bridge are rigid and the shape of the bridge's cross-section is unchanged during vibration. The rail irregularity is negligible. (2) In order to understand the dynamic responses of the passenger cars, the train is modeled as a periodic series of planar moving forces or moving suspension masses. The train loads are applied at the centerline of the beam and move along the longitudinal direction with a constant speed.

2.2. Equations of motion for bridge-PTMD system under train loads

Let a s.d.o.f. PTMD be installed at a beam-like bridge with length L at position $x = x_s$, as shown in Fig. 1. When a train, consisting of N_v number of moving loads, is passing over the bridge with constant speed v, the governing equations for the bridge-PTMD system are given as follows: (1) the vertical motion of the bridge at mass center,

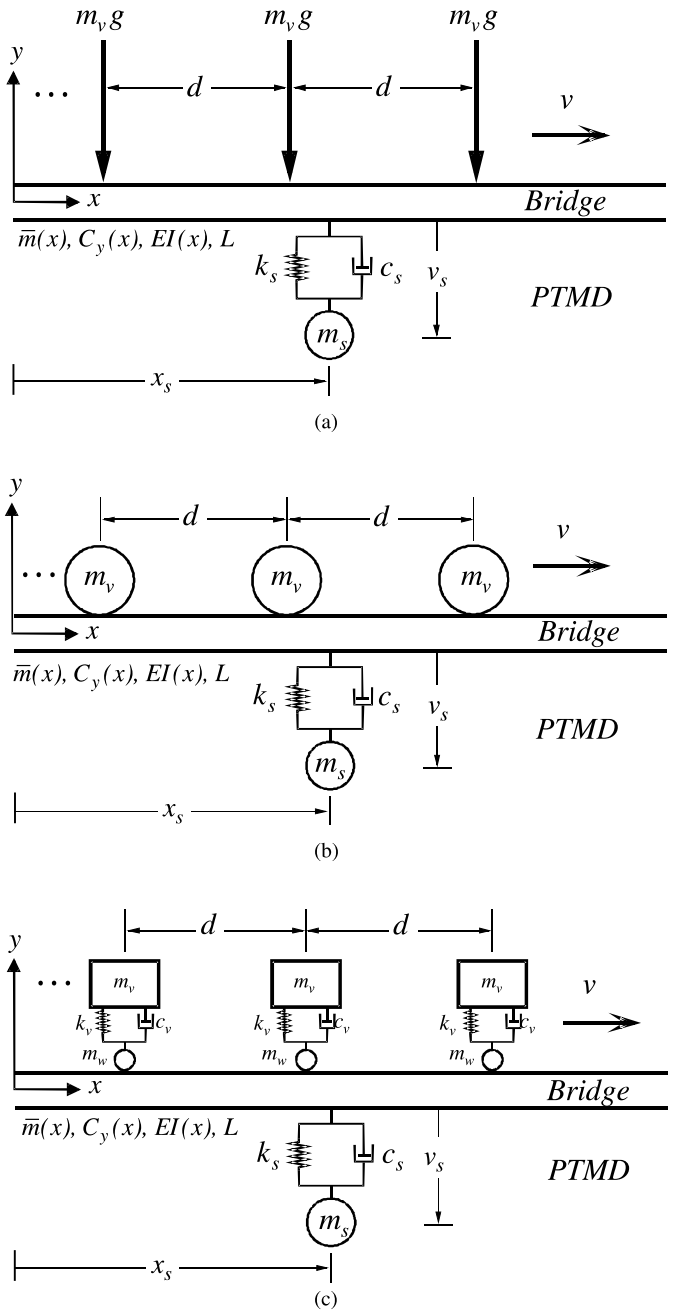

Fig. 1. Bridges combined with PTMD under train loads simulated as: (a) moving force model; (b) moving mass model; (c) moving suspension mass model.

$$\bar{\boldsymbol{m}}(x)\frac{\partial^2 y(x,t)}{\partial t^2} + C_y(x)\frac{\partial y(x,t)}{\partial t} + \frac{\partial^2 y(x,t)}{\partial x^2}\left[EI(x)\frac{\partial^2 y(x,t)}{\partial x^2}\right] = P_{\mathrm{b}}(x,t) \tag{1a}$$

where the train loading function

$$P_{\mathrm{b}}(x,t) = -\sum_{k=1}^{N_v} p_k \delta[x - v(t-t_k)]H(t,t_k) + \{k_{\mathrm{s}}[z_s - y(x_s,t)] + c_s[\dot{z}_s - \dot{y}(x_s,t)]\} \cdot \delta(x - x_s) \tag{1b}$$

and $H(t,t_k) = U(t-t_k) - U[t-(t+v/L)]$; $U(-)$ and $\delta(-)$ represent the unit step function and the Dirac delta function, respectively, which are defined as

$$\int_{-\infty}^{\infty} \delta(x)\,\mathrm{d}x = \begin{cases} 1, & x = 0 \\ 0, & x \neq 0 \end{cases} \tag{2}$$

$$U(t) = \begin{cases} 1, & t \geqslant 0 \\ 0, & t < 0 \end{cases} \tag{3}$$

(2) the vertical motion of PTMD,

$$m_s\ddot{z}_s(t) + c_s[\dot{z}_s(t) - \dot{y}(x_s,t)] + k_{\mathrm{s}}[z_s(t) - y(x_s,t)] = 0 \tag{4}$$

In Eqs. (1) and (4), $\bar{m}(x)$, $C_y(x)$ and $EI(x)$ represent the mass per unit length, damping coefficient of the flexural motion and rigidity of the flexural motion of the bridge at section x, respectively. m_s, c_s and k_{s} represent the mass, damping coefficient, stiffness coefficient of the PTMD. $y(x,t)$ and $z_s(t)$ indicate the vertical displacement of the bridge and the PTMD. In Eq. (1b), the expression for the train load, $P_{\mathrm{b}}(x,t)$, was proposed by Yang et al. (1997), where p_k is the magnitude of kth load and t_k denotes the time when the kth load reaches the bridge. To calculate the train loads, $\delta(x)$ and $U(t)$ are introduced to locate the position of each load on the bridge. It is easily recognized that, the second term of the right hand side of the summation sign in Eq. (1b) determines the location of kth load on the bridge, whereas the third term determines whether the kth load is on the bridge or not. It should be noted that the value of p_k is dependent upon the train model. For the moving force model, as shown in Fig. 1(a),

$$p_k = m_{v_k} g \tag{5a}$$

which is the weight of the kth load. If a moving mass model (Fig. 1(b)) and moving suspension mass model (Fig. 1(c)) are used, p_k is written as

$$p_k = m_{v_k} \cdot \{g + \ddot{y}[v(t-t_k),t]\} \tag{5b}$$

and

$$p_k = m_{v_k} \cdot [g + \ddot{z}_v(t)] \tag{5c}$$

respectively, where m_{v_k} and $z_v(t)$ are the mass and the vertical displacement of the kth train load. Comparing the three train models, it is observed that the inertial force of the vehicle is neglected in the first model and taken into account in the other models in different manners. Actually, the moving force and moving mass models are particular cases of moving suspension mass model. When the suspension stiffness is rigid, the vehicle acceleration, $\ddot{z}_v(t)$, is equal to the acceleration where the vehicle is located, and thus Eq. (5c) will turn out to be Eq. (5b). On the other hand, when the suspension stiffness is very soft, $\ddot{z}_v(t)$ will approach to zero theoretically. Eq. (5c) will be equal to Eq. (5a), which represents the moving force model. Obviously, the vehicular movement will alter the dynamic characteristics of the entire system since the train loads are relative to the bridge response as precise models are employed.

2.3. Modal decoupling to solve partial differential equations

To analytically solve Eqs. (1) and (4), modal analysis was employed to separate the governing parameters. The vertical displacement $y(x,t)$ can be expressed as the product of the beam vertical vibration

mode shape function involving only the spatial coordinate, x, and modal response functions involving the variable time, t. Using the concept of modal superposition, $y(x,t)$ can be represented as

$$y(x,t) = \sum_{j=1}^{N} \phi_j(x)\eta_j(t) = \mathbf{\Phi}^{\mathrm{T}}(x)\boldsymbol{\eta}(t) \tag{6}$$

where N is the number of modes to be considered for the bridge. $\mathbf{\Phi}(x)$ represents the mode-shape matrix and $\boldsymbol{\eta}(t)$ is the modal-response vector. Let $v_s(t) = z_s(t) - y(x_s,t)$ be the PTMD stroke (i.e., the PTMD displacement relative to the bridge where the PTMD is located). Substituting Eq. (6) into Eq. (1), and pre-multiplying $\mathbf{\Phi}(x)$ and integrating from 0 to L at each side of Eq. (1), it becomes

$$\left[\int_0^L \mathbf{\Phi}(x)\bar{m}(x)\mathbf{\Phi}^{\mathrm{T}}(x)\,\mathrm{d}x\right]\ddot{\boldsymbol{\eta}}(t) + \left[\int_0^L \mathbf{\Phi}(x)C_y(x)\mathbf{\Phi}^{\mathrm{T}}(x)\,\mathrm{d}x\right]\dot{\boldsymbol{\eta}}(t) + \left[\int_0^L \mathbf{\Phi}''(x)EI(x)\mathbf{\Phi}''^{\mathrm{T}}(x)\,\mathrm{d}x\right]\boldsymbol{\eta}(t)$$
$$= -\sum_{k=1}^{N_v} p_k\mathbf{\Phi}[v(t-t_k)]H(t,t_k) + \mathbf{\Phi}(x_s)(c_s\dot{v}_s + k_s v_s) \tag{7a}$$

or in matrix form as

$$\mathbf{M}_{\mathrm{b}}\ddot{\boldsymbol{\eta}}(t) + \mathbf{C}_{\mathrm{b}}\dot{\boldsymbol{\eta}}(t) + \mathbf{K}_{\mathrm{b}}\boldsymbol{\eta}(t) = \mathbf{F}_{\mathrm{b}}(t) + \mathbf{\Phi}(x_s)(c_s\dot{v}_s + k_s v_s) \tag{7b}$$

where $\mathbf{M}_{\mathrm{b}}$, $\mathbf{C}_{\mathrm{b}}$ and $\mathbf{K}_{\mathrm{b}}$ are N by N matrices representing the modal mass, damping and stiffness matrices of the bridge vertical motions. It is well known that these matrices become diagonal after the orthogonality of $\mathbf{\Phi}(x)$ is applied. Therefore, Eq. (7) can be decoupled into N number of modes and the jth modal equation of motion is expressed as

$$m_{\mathrm{b}}\ddot{\eta}_j(t) + c_{\mathrm{b}}\dot{\eta}_j(t) + k_{\mathrm{b}}\eta_j(t) = F_{\mathrm{b}_j}(t) + \phi_j(x_s)(c_s\dot{v}_s + k_s v_s) \tag{8a}$$

where

$$m_{\mathrm{b}_j} = \int_0^L \bar{m}(x)\phi_j^2(x)\,\mathrm{d}x, \quad c_{\mathrm{b}_j} = \int_0^L C_y(x)\phi_j^2(x)\,\mathrm{d}x, \quad k_{\mathrm{b}_j} = \int_0^L EI(x)[\phi_j''(x)]^2\,\mathrm{d}x \tag{8b}$$

and

$$F_{\mathrm{b}_j}(t) = -\sum_{k=1}^{N_v} p_k\phi_j(vt - vt_k)H(t,t_k) \tag{8c}$$

Moreover, the coordinate in Eq. (4) can be rearranged into the PTMD stroke as

$$m_s\ddot{v}_s(t) + c_s\dot{v}_s(t) + k_s v_s(t) = -m_s\ddot{y}(x_s,t) \tag{9}$$

Substituting Eq. (6) into Eq. (9), it becomes

$$m_s\ddot{v}_s(t) + c_s\dot{v}_s(t) + k_s v_s(t) = -m_s\mathbf{\Phi}^{\mathrm{T}}(x_s)\ddot{\boldsymbol{\eta}}(t) \tag{10}$$

Combining Eqs. (7b) and (10), the coupled equations of motion in modal space are given in matrix form as

$$\begin{bmatrix} \mathbf{M}_{\mathrm{b}} & \mathbf{0} \\ m_s\mathbf{\Phi}^{\mathrm{T}}(x_s) & m_s \end{bmatrix}\begin{Bmatrix} \ddot{\boldsymbol{\eta}}(t) \\ \ddot{v}_s(t) \end{Bmatrix} + \begin{bmatrix} \mathbf{C}_{\mathrm{b}} & -c_s\mathbf{\Phi}(x_s) \\ \mathbf{0}^{\mathrm{T}} & c_s \end{bmatrix}\begin{Bmatrix} \dot{\boldsymbol{\eta}}(t) \\ \dot{v}_s(t) \end{Bmatrix} + \begin{bmatrix} \mathbf{K}_{\mathrm{b}} & -k_s\mathbf{\Phi}(x_s) \\ \mathbf{0}^{\mathrm{T}} & k_s \end{bmatrix}\begin{Bmatrix} \boldsymbol{\eta}(t) \\ v_s(t) \end{Bmatrix} = \begin{Bmatrix} \mathbf{F}_{\mathrm{b}}(t) \\ 0 \end{Bmatrix} \tag{11}$$

where $\mathbf{0}$ represents a zero vector. In this study, direct numerical integration is applied to solve Eq. (11), and the vertical displacement response of the bridge, $y(x,t)$, is then calculated from Eq. (6).

3. Dynamic characteristics of bridge and train

It is noted that a train is generally composed of a series of moving cars with the same properties. Such an excitation acts like a steady continuous impact upon a bridge when the train is moving at a constant speed. The vibration frequency of the bridge would then be stationary at a specified value. This situation is different from that of a highway bridge subjected to single car load in a short time. Therefore, it is interesting to understand the properties of train loads so that the dynamic characteristics of the bridges under train loads can be predicted.

3.1. Resonant speeds

Assuming that a bridge is constructed with simple supports. It's mode-shape function, $\mathbf{\Phi}(x)$, can be expressed as

$$\mathbf{\Phi}(x) = \left\{ \sin\tfrac{\pi x}{L} \quad \sin\tfrac{2\pi x}{L} \quad \cdots \quad \sin\tfrac{j\pi x}{L} \quad \cdots \right\} \tag{12}$$

With this definition, the spectrum of the jth modal train load, $F_{\mathrm{b}_j}(\omega)$, could be found through taking the Fourier transform of $F_{\mathrm{b}_j}(t)$ as

$$\begin{aligned} F_{\mathrm{b}_j}(\omega) &= \frac{1}{2\pi}\int_{-\infty}^{\infty} F_{\mathrm{b}_j}(t)\mathrm{e}^{-\mathrm{i}\omega t}\,\mathrm{d}t = \frac{1}{2\pi}\int_{-\infty}^{\infty}\left\{ -\sum_{k=1}^{N_v} p_k \phi_j(vt - vt_k)H(t,t_k)\right\}\mathrm{d}t \\ &= -\frac{1}{2\pi}\sum_{k=1}^{N_v}\left\{ \int_{-\infty}^{\infty} p_k\left[\sin\frac{j\pi v(t-t_k)}{L}\right]H(t,t_k)\,\mathrm{d}t\right\} \end{aligned} \tag{13}$$

As stated earlier, if the interactive system model was employed, the value of p_k would be related to both the bridge and the vehicle responses. In order to explore the train load analytically, assuming that each moving load has the same magnitude ($p_1 = p_2 = \cdots = p_k = p_0$) and same spacing d, then the analytical expression of $F_{\mathrm{b}_j}(\omega)$ for a simply supported bridge can be derived as

$$F_{\mathrm{b}_j}(\omega) = \frac{\frac{p_0\pi v j}{\omega^2 L}}{1-\left(\frac{j\pi v}{\omega L}\right)^2}\left[\frac{1}{2} + \frac{\sin\left(\frac{\omega d}{2v}N_v - \frac{\omega d}{2v}\right)}{\sin\left(\frac{\omega d}{2v}\right)}\right]\cdot\left[(-1)^j\cdot\mathrm{e}^{-\mathrm{i}\omega L/v} - 1\right] \tag{14}$$

It was found that the value of $F_{\mathrm{b}_j}(\omega)$ would be large as $\sin(\omega d/2v) \approx 0$ or as $\omega = 2\pi n v/d$ ($n = 1, 2, 3, \ldots$), where v/d is the impact frequency of the wheel loads to the bridge. For instance, for a series of moving forces with $d = 25$ m and fifty loads passing a 28.4 m bridge at a speed of $v = 82$ km/h, the magnitude of the spectrum of the first modal force, $|F_{\mathrm{b}_1}(\omega)|$, is illustrated in Fig. 2(a). It is obviously seen that there exists peaks when the excitation frequency, ω, is equal to $2\pi v/d = (0.91$ Hz), $4\pi v/d (= 1.82$ Hz), $6\pi v/d (= 2.73$ Hz), …, etc., as expected for $N_v = 50$. In this condition, if the modal frequency of the bridge, ω_j, is close to the multiple of the impact frequency of the moving loads, the resonant effect will occur. In other words, the bridge will undergo resonant responses when

$$v = v_c = \frac{\omega_j d}{2n\pi} \tag{15}$$

where $n = 1, 2, 3, \ldots$ These speeds are called the resonant speeds. In Eq. (14), it is also shown that the resonant condition occurs not only at high train speed but also at medium train speeds. Examination of Eq. (14) indicates that other critical conditions occur when $1 - (j\pi v/\omega L)^2 = 0$ or $\omega = n\pi v/L$. That is,

$$v = \frac{\omega_j L}{n\pi} \tag{16}$$

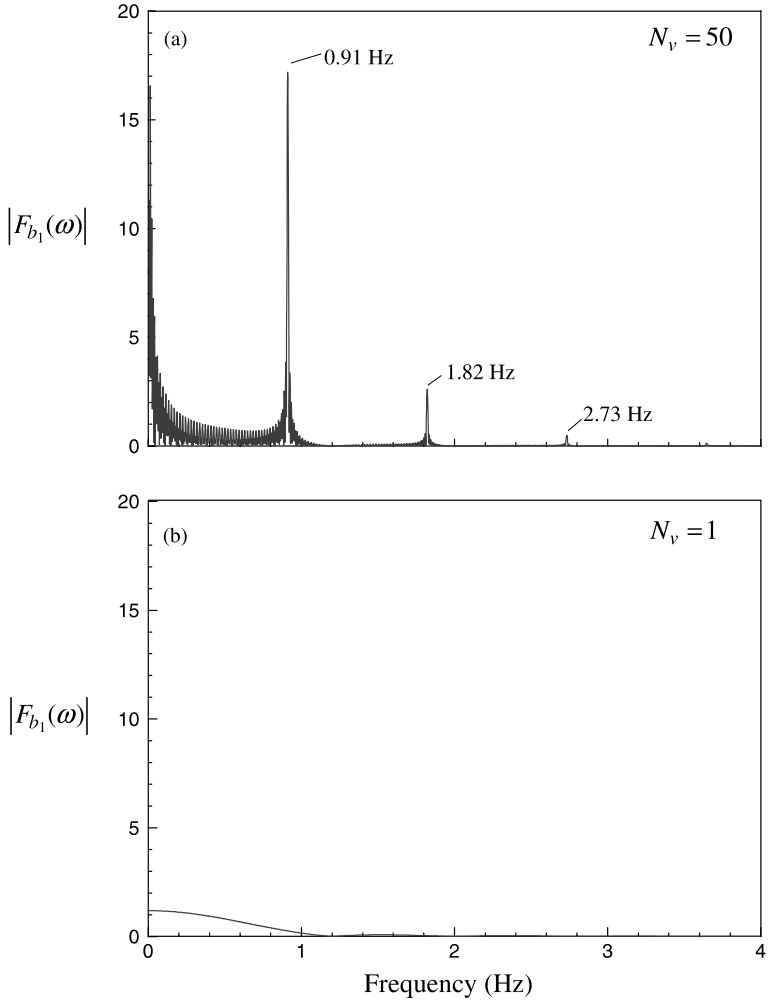

Fig. 2. Fourier transform of the first modal train load with various numbers of loads: (a) fifty loads; (b) one load.

Compared with Eq. (15), one can observe that the major critical condition (for $n = 1$) is only encountered when the train speed is several times the first resonant speed. This seems to be impossible for general HSR bridges. These findings are the same as those found by Yang et al. (1997). The conditions in Fig. 2(b) are same as those in Fig. 2(a) except that the number of moving loads is one. Apparently, there does not exist any obvious excitation frequency. Like a single car passing through a bridge, no resonant response will be produced.

3.2. Influence of train models

From Eq. (15), it is seen that the resonant speeds of a train are dependent upon two factors, the modal frequencies of the bridge, ω_j, and the load spacing of the train, d. As stated earlier, the interaction between the bridge and train will exist as precise train models are applied. For example, applying a moving mass

model for the train (using Eqs. (5b) and (6)) and without the installation of PTMD, the equation of motion of the bridge, Eq. (7), becomes

$$\mathbf{M}_{\mathrm{b}}\ddot{\boldsymbol{\eta}}(t)+\mathbf{C}_{\mathrm{b}}\dot{\boldsymbol{\eta}}(t)+\mathbf{K}_{\mathrm{b}}\boldsymbol{\eta}(t)=-\sum_{k=1}^{N_v}m_v\left\{g+\boldsymbol{\Phi}^{\mathrm{T}}[v(t-t_k)]\ddot{\boldsymbol{\eta}}(t)\right\}\boldsymbol{\Phi}[v(t-t_k)]H(t,t_k) \tag{17a}$$

or

$$[\mathbf{M}_{\mathrm{b}}+\mathbf{M}'_{\mathrm{b}}(t)]\ddot{\boldsymbol{\eta}}(t)+\mathbf{C}_{\mathrm{b}}\dot{\boldsymbol{\eta}}(t)+\mathbf{K}_{\mathrm{b}}\boldsymbol{\eta}(t)=-\sum_{k=1}^{N_v}m_v g\boldsymbol{\Phi}[v(t-t_k)]H(t,t_k) \tag{17b}$$

where $\mathbf{M}'_{\mathrm{b}}(t)=\sum_{k=1}^{N_v}m_v\boldsymbol{\Phi}^{\mathrm{T}}[v(t-t_k)]\boldsymbol{\Phi}[v(t-t_k)]H(t,t_k)$. It is apparent that the mass matrix of the bridge system will be altered because of the addition of the train. Moreover, the variation in the mass varies with time. This means that the modal frequency of the bridge will change with time during the passage of the train. Fig. 3 shows the time variation of first modal frequency of the bridge, B2 (whose properties are shown in Table 1), subjected to a French T.G.V. train (whose properties are shown in Table 2) with certain speed simulated as a moving mass model. Since the overall mass of the bridge system increases as the train moves onto the bridge, the system natural frequencies are smaller than their original values. Moreover, the variation of the first modal frequency at different time is small and almost stable at an average value, $(\omega_1)_{\mathrm{avg}}$, as the train steadily acts on the bridge. This phenomenon will lead to a change in the resonant train speeds. For various train speeds, the corresponding values of $(\omega_1)_{\mathrm{avg}}$ (solid line) are illustrated in Fig. 4. It is shown that the greater train speed, the smaller $(\omega_1)_{\mathrm{avg}}$, but their differences are very small. According to Eq. (15), the line relating the first modal frequency of the bridge-train system and the main resonant train speed ($j=1$ and $n=1$) is also illustrated in Fig. 4. This line intersects $(\omega_1)_0$ and $(\omega_1)_{\mathrm{avg}}$ at two points, which abscissas denote the resonant train speeds (v_c and v'_c) for moving force and moving mass train models, respectively. It is seen that v'_c is smaller than v_c, because of $(\omega_1)_{\mathrm{avg}}<(\omega_1)_0$. But, their differences are about 2.5%. It indicates that the application of different train models does not lead to significant change of resonant train speeds.

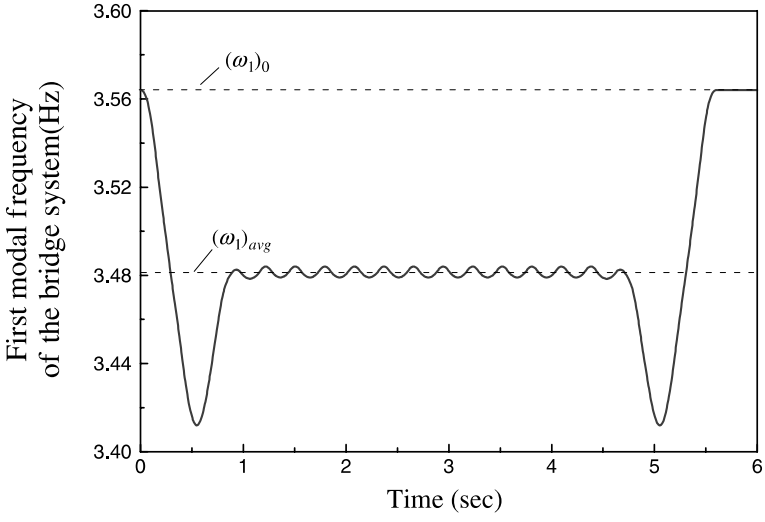

Fig. 3. Time variation of the first modal frequency of the bridge B2 under a French T.G.V. train simulated as moving mass model; $(\omega_1)_0$: the original value; $(\omega_1)_{\mathrm{avg}}$: the average value as the train steadily travels over bridge.

Table 1
Properties of two THSR bridges

Properties	Bridge B1 ($L = 30$ m)	Bridge B2 ($L = 40$ m)
E (t/m^2)	2.83×10^6	2.87×10^6
I (m^4)	7.84	17.90
$\bar{m}$ (t/m)	41.74	38.24
ξ_j (%)	2.5	2.5
ω_1 (Hz)	4.64	3.56

Table 2
Properties of German I.C.E., Japanese S.K.S. and French T.G.V. HSR trains

Train properties	I.C.E.	S.K.S.	T.G.V.
No. of bogie	52	64	52
Car spacing, d (m)	26.4	25.0	18.7
$(v_c)_{n=1}$ (km/h) Bridge B1	440	418	311
$(v_c)_{n=2}$ (km/h) Bridge B1	220	209	156
$(v_c)_{n=1}$ (km/h) Bridge B2	338	320	240
$(v_c)_{n=2}$ (km/h) Bridge B2	169	160	120
m_v (kg)	27,000	20,875	27,000
c_v (N s/m)	22,700	90,200	96,700
k_v (N/m)	660,000	530,000	664,000
m_b (kg)	3000	3040	3000
I_b (kg m^2)	4000	3930	4000
c_b (N s/m)	78,400	78,400	78,400
k_b (N/m)	2,360,000	2,360,000	2,360,000
m_w (kg)	1800	1780	1800
l_w (m)	1.5	1.25	1.5

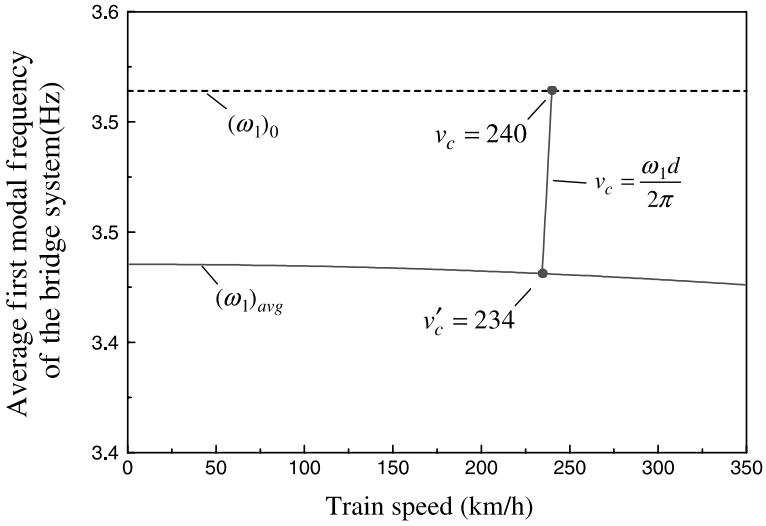

Fig. 4. Average first modal frequency of the bridge system versus train speed and the change of resonant train speed for a T.G.V. train traveling over bridge B2.

4. Optimal passive tuned mass dampers

The PTMD concept dates back to 1909 (Frahm, 1911). Since then, much research has been carried out to examine its effectiveness for various dynamic load applications. This device is installed to absorb the energy transmitted from the primary structure by tuning its frequency to the structural frequency without additional power. The success of such a system in reducing wind-excited structural responses is now well established. However, because of the complex characteristics of earthquake excitations, there still has not been a general agreement on the effectiveness of PTMD systems in suppressing seismic responses. The PTMD effectiveness for suppressing traffic responses has also not been clearly investigated and confirmed.

4.1. Design philosophy and control effectiveness of PTMD

The design philosophy for PTMD generally is to alter the characteristics of the primary structure so that the system is applicable to the changes in external excitations. In order to understand this principle, one can use the transfer function to examine the PTMD. Fig. 5 shows the typical transfer function of the specified mode of a structure with and without PTMD, designed for seismic response control based on the optimization procedure by Lin et al. (1994). It is seen that these two curves intersect at points P and Q. It is known that the positions of P and Q vary with the PTMD's natural frequency, ω_s, and their elevations are independent of the PTMD's damping ratio, ξ_s. It is also seen that the transfer function of a structure with PTMD decreases in the frequencies between P and Q (operating range), but does not reduce or may even amplify in the other frequencies. Thus, it is expected that the PTMD will not produce vibration reduction unless the frequency content of the excitations is within the operating range. Otherwise, the PTMD will be ineffective. This phenomenon can be verified in the time domain using two s.d.o.f. structures A ($\omega_p = 1.13$ Hz, $\xi_p = 2\%$) and B ($\omega_p = 3.0$ Hz, $\xi_p = 2\%$) subjected to the horizontal earthquake acceleration recorded at the campus of National Chung-Hsing University (called NCHU record) during the 1999 Taiwan Chi-Chi earthquake. Fig. 6 shows the Fourier amplitude spectrum of the NCHU earthquake record and the operating ranges of structures A and B. It is clearly seen that the major frequency content of the exciting

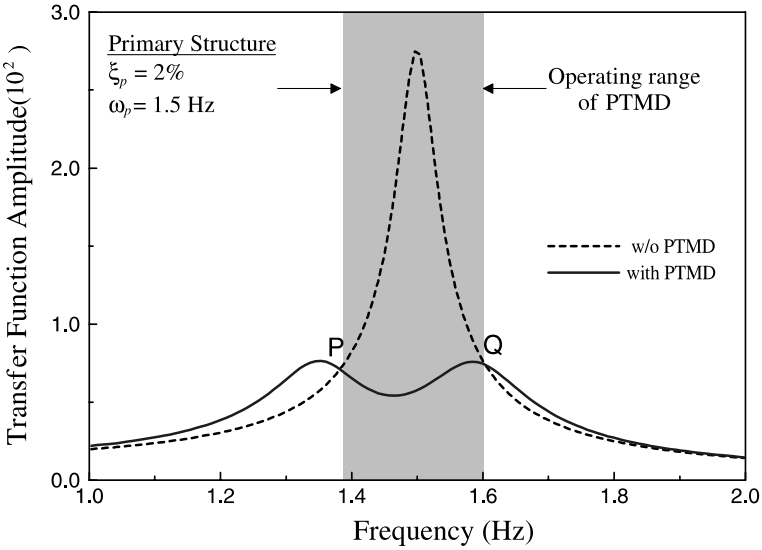

Fig. 5. Typical transfer function of a structure with and without optimal PTMD.

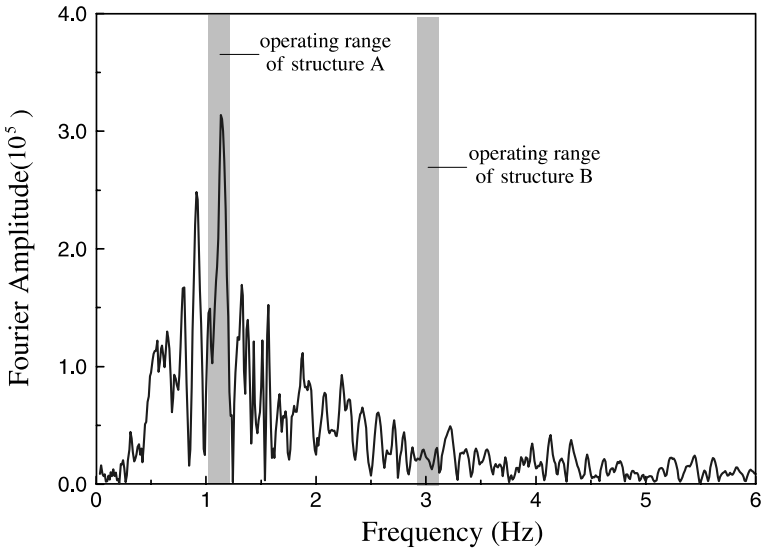

Fig. 6. Fourier amplitude spectrum of the NCHU record during 1999 Taiwan Chi-Chi earthquake and the PTMD operating range for structures A and B.

earthquake falls in the operating range of structure A, but not in that of structure B. The structural displacement time histories are illustrated in Fig. 7(a) and (b) which show that the PTMD performance is excellent for structure A, but is not good for structure B, as expected in the frequency domain. This result implies that the PTMD effectiveness is highly frequency-dependent. It operates efficiently only under resonant conditions. In previous researches, PTMD was intuitively thought to be an ineffective seismic control device because of this phenomenon. However, although PTMD is less useful outside resonant conditions, the structural response is small in this situation. Therefore, the PTMD is a useful vibration control device in reducing the "excessive" responses, which occur during resonant conditions. As stated in Section 3.1, it is known that the spectrum of train loads is a narrow-banded and well separated like a simple harmonic force, and the resonant peaks occur when the train is traveling at resonant speeds. Therefore, the PTMD can be expected to be able to reduce the bridge responses under these conditions.

4.2. Optimal PTMD parameters for simply supported bridges

After the equations of motion for the bridge-PTMD system are established, the PTMD parameters are determined so that the bridge responses are smaller than those without the installation of PTMD. Since the train factors, such as speed, weight, axial distance, etc., are all unknown, it is usually not desired to include these uncertainties into the PTMD parameter determination. The main goal in designing a single PTMD is to alter only the dynamic characteristics of the bridge.

Since a single PTMD system has a single natural frequency, only one vibration mode of the bridge can be controlled. According to Eq. (11), selecting the jth mode of the bridge as controlled mode and combining it with the PTMD, the equation of motion for the system could be given in the matrix form as

$$\begin{bmatrix} m_{\mathrm{b}_j} & 0 \\ m_s\phi_j(x_s) & m_s \end{bmatrix} \begin{Bmatrix} \ddot{\eta}_j(t) \\ \ddot{v}_s(t) \end{Bmatrix} + \begin{bmatrix} c_{\mathrm{b}_j} & -c_s\phi_j(x_s) \\ 0 & c_s \end{bmatrix} \begin{Bmatrix} \dot{\eta}_j(t) \\ \dot{v}_s(t) \end{Bmatrix} + \begin{bmatrix} k_{\mathrm{b}_j} & -k_{\mathrm{s}}\phi_j(x_s) \\ 0 & k_{\mathrm{s}} \end{bmatrix} \begin{Bmatrix} \eta_j(t) \\ v_s(t) \end{Bmatrix} = \begin{Bmatrix} F_{\mathrm{b}_j}(t) \\ 0 \end{Bmatrix} \tag{18}$$

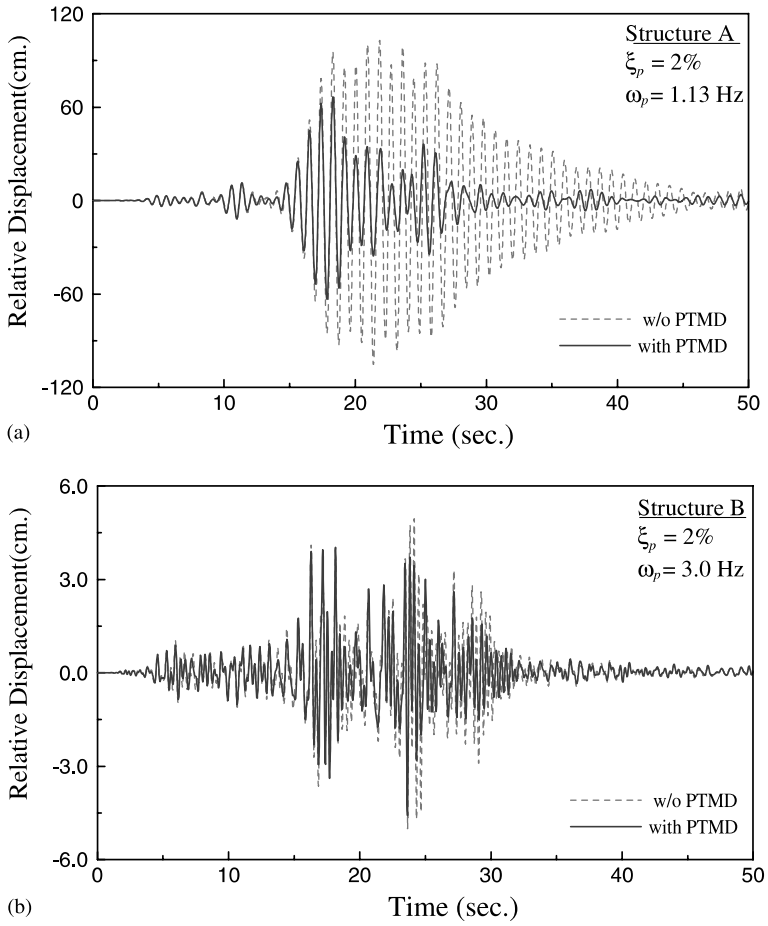

Fig. 7. Relative displacement time history of structures A and B with and without PTMD under the NCHU record of 1999 Taiwan Chi-Chi earthquake.

Dividing the first and second rows by m_{b_j} and m_s respectively, Eq. (18) becomes

$$\begin{bmatrix} 1 & 0 \\ \phi_j(x_s) & 1 \end{bmatrix} \begin{Bmatrix} \ddot{\eta}_j(t) \\ \ddot{v}_s(t) \end{Bmatrix} + \begin{bmatrix} 2\xi_j\omega_j & -2\xi_s\omega_s u_{s_j} \\ 0 & 2\xi_s\omega_s \end{bmatrix} \begin{Bmatrix} \dot{\eta}_j(t) \\ \dot{v}_s(t) \end{Bmatrix} + \begin{bmatrix} \omega_j & -\omega_s^2 u_{s_j} \\ 0 & \omega_s^2 \end{bmatrix} \begin{Bmatrix} \eta_j(t) \\ v_s(t) \end{Bmatrix} = \begin{Bmatrix} 1 \\ 0 \end{Bmatrix} F_{\mathrm{b}_j}(t)/m_{\mathrm{b}_j} \tag{19a}$$

or

$$\mathbf{M}\ddot{\mathbf{Z}}(t) + \mathbf{C}\dot{\mathbf{Z}}(t) + \mathbf{K}\mathbf{Z}(t) = \mathbf{\Gamma}F(t), \tag{19b}$$

where ξ_s and ω_s represent the damping ratio and natural frequency of the PTMD, respectively, whereas $\mu_{s_j} = \phi_j(x_s)m_s/m_{\mathrm{b}_j}$ means the modal mass ratio of the PTMD. Taking the Fourier transform of Eq. (19) yields

$$\mathbf{Z}(\omega) = (-\omega^2\mathbf{M} + \mathrm{i}\omega\mathbf{C} + \mathbf{K})^{-1}\mathbf{\Gamma}F(\omega) = \mathbf{A}^{-1}\mathbf{\Gamma}F(\omega) = \begin{Bmatrix} H_{\eta_j F}(\omega) \\ H_{v_s F}(\omega) \end{Bmatrix} F(\omega) \tag{20}$$

where

$$\mathbf{A} = \begin{bmatrix} -\omega^2 + \mathrm{i}\omega(2\xi_j\omega_j) + \omega_j^2 & -\mathrm{i}\omega(2\xi_s\omega_s\mu_{s_j}) - \omega_s^2\mu_{s_j} \\ -\omega^2\phi_j(x_s) & -\omega^2 + \mathrm{i}\omega(2\xi_s\omega_s) + \omega_s^2 \end{bmatrix}$$

The functions $H_{\eta_j F}(\omega)$ and $H_{v_s F}(\omega)$ represent the transfer functions of the jth modal displacement of the bridge and the PTMD stroke corresponding to the modal train load $F(\omega)$, respectively. When a train travels at a constant speed, the main excitation frequency is usually narrow banded, as shown in Fig. 2(a). Therefore, the suppression of peak value of the transfer function is important rather than the entire area of the transfer function. Considering the cases of a bridge with and without the installation of PTMD, a response ratio is defined as

$$R_{dv_j} = \frac{\text{peak value of } |H_{\eta_j F}(\omega)|_{\text{PTMD}}}{\text{peak value of } |H_{\eta_j F}(\omega)|_{\text{NOPTMD}}} \tag{21}$$

to evaluate the vibration control effectiveness of PTMD. The index R_{dv_j} is a function of ξ_j, $\phi_j(x_s)$ (bridge parameters), μ_{s_j}, ξ_s and r_{f_j} (PTMD parameters), where $r_{f_j} = \omega_s/\omega_j$ is the modal frequency ratio. For given values of ξ_j and $\phi_j(x_s)$, the optimal PTMD parameters can be obtained by differentiating R_{dv_j} with respect to r_{f_j}, ξ_s and μ_{s_j}, and equating to zero, respectively, to minimize R_{dv_j}. These values may be found by solving the following equations simultaneously

$$\frac{\partial R_{dv_j}}{\partial \mu_{s_j}} = 0, \quad \frac{\partial R_{dv_j}}{\partial \xi_s} = 0, \quad \frac{\partial R_{dv_j}}{\partial r_{f_j}} = 0 \tag{22}$$

In general, the bridge parameters are determined through other approaches, for example, by system identification techniques for existing bridges. The optimal location, x_s, for the placement of PTMD is at the place where the controlled mode-shape value is maximal (Lin et al., 1994), that is, at the middle of a span (i.e., $x_s = 0.5L$) for simply supported bridges when the first mode is to be controlled. Meanwhile, in practice, the modal mass ratio, μ_{s_j}, is generally assigned by considering both economy and the bridge capacity, and finally, the optimal set of (r_{f_j}, ξ_s) are found through solving the remaining two equations in (22).

5. Numerical verifications

Based on the theoretical derivations described previously, some numerical investigations are performed in this section. The bridges B1 and B2 whose properties listed in Table 1, which are proposed for THSR (Lin, 1993), are used for verifying the PTMD control effectiveness. Bridge B1 represents a general bridge with a length of 30 m, whereas Bridge B2 is a medium long bridge with a length of 40 m, as shown in Fig. 8. Both bridges are constructed as simply supported bridges with a constant cross section area of box girder inside which a single PTMD is to be installed. Three various trains, French T.G.V., German I.C.E., and Japanese S.K.S., shown in Fig. 9, are used as the external moving loads acting on the bridges. According to the THSR design specifications, the vertical displacement, acceleration and end rotation of the bridge, and the vertical acceleration of the train should be limited to assure the safety and the comfort of passengers. The reductions of the four dynamic responses of the bridge due to the installation of proposed optimal PTMD will be clearly illustrated in this section. In addition, the PTMD detuning effect, resulting from the interaction between the vehicle and the bridge, on the PTMD control effectiveness will also be extensively examined.

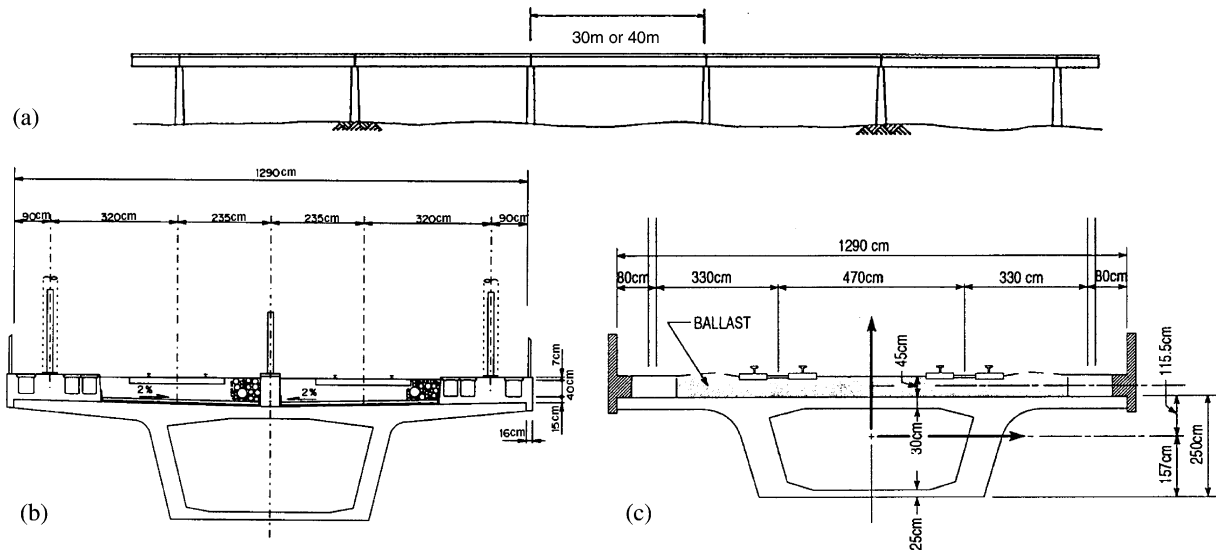

Fig. 8. Configurations of proposed Taiwan high-speed railway bridge: (a) viewed along the transverse section plane; (b) section profile of bridge with thirty meters span; (c) section profile of bridge with forty meters span.

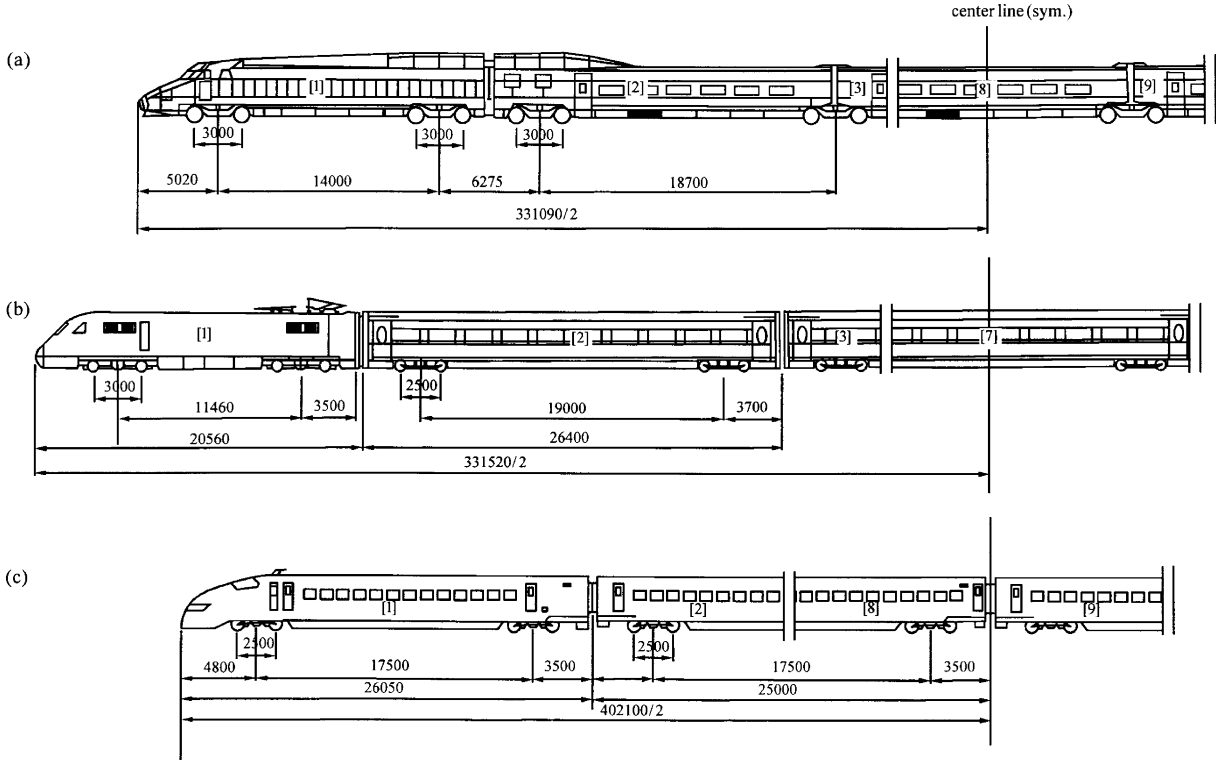

Fig. 9. Axle arrangements of three HSR trains: (a) French T.G.V.; (b) German I.C.E.; (c) Japanese S.K.S. (unit: mm).

5.1. PTMD control effectiveness for THSR bridges under train loads

Since the space between two axles (3 m) is not too small compared with the length of B1 (30 m), two loads for two axles are modeled to calculate the dynamic responses of bridge-PTMD system and French T.G.V., German I.C.E., and Japanese S.K.S. trains. Fig. 10 illustrates the train load model which consists of a mass-spring-dashpot system (m_v, k_v, c_v) to represent one half of a train car, one bogie system with two d.o.f.s. (z_b, θ_b), and two wheel sets (m_w). Their physical properties used in this paper are listed in Table 2. According to the car spacing of each train and the modal frequencies of bridges B1 and B2, the corresponding resonant train speeds ($j = 1$ and $n = 1, 2$) for each bridge are calculated and also shown in Table 2. It is found that the main resonant train speeds ($j = 1$ and $n = 1$) for bridge B1 are larger than the design train speed of 350 km/h except for the French T.G.V. since bridge B1 is more rigid than bridge B2. The PTMD is designed to control the first-mode response that dominates the total responses of bridge and train systems and is installed at the middle of the bridge where the mode-shape value is maximal. The modal mass ratio μ_{s_1} is selected to be 0.5% and the corresponding optimal PTMD parameters based on the optimal design procedures and criteria in Section 4 are calculated and listed in Table 3. To investigate the PTMD control effectiveness, the maximal values of the four dynamic responses, which were mentioned previously, for bridges with and without PTMD within the design train speed (350 km/h) are presented in Tables 4 and 5. Because the main resonant train speeds for bridge B1 are larger than the design speed, the maximal bridge responses are not dominant by the resonant responses that the PTMD is expected to suppress. Therefore, the response reductions for bridge B1 and the trains due to the PTMD installation are quite small. Moreover, parts of the dynamic responses are even amplified for the cases of the I.C.E. and S.K.S. trains as we expected. However, it is seen that the response values shown in Table 4 are very small and far from the design limitations. In this situation, the vibration control devices are actually not necessary.

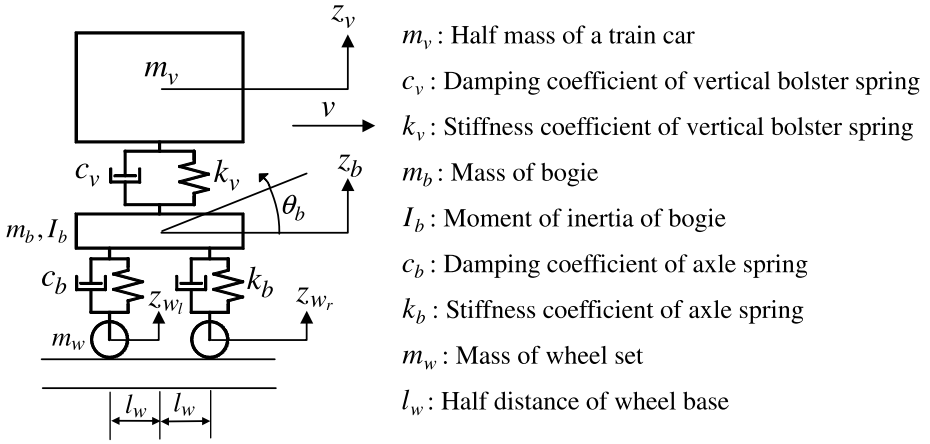

Fig. 10. Illustration of train load model.

Table 3
Optimal PTMD parameters for two THSR bridges

PTMD parameters	Mass (kg) m_s ($\mu_{s_1} = 0.5\%$)	Damping (N s/m) c_s ($\xi_s = 5\%$)	Stiffness (N/m) k_s ($r_f = 0.991$)
For bridge B1	5802	16904	4.84×10^6
For bridge B2	7648	16978	3.77×10^6

Table 4
Maximal responses of trains and bridge B1 with and without PTMD

Train type	PTMD condition	Maximal vertical displacement at midspan (cm)	Maximal vertical acceleration at midspan (g)	Maximal rotation at right end (10^{-4} radian)	Maximal vertical acceleration at bogie (g)
I.C.E.	Without PTMD	0.200	0.080	2.26	0.005
	With PTMD	0.200	0.076	2.27	0.005
		(0.0%)	(5.0%)	(−0.4%)	(0.0%)
S.K.S.	Without PTMD	0.166	0.074	1.87	0.010
	With PTMD	0.167	0.072	1.90	0.010
		(−0.6%)	(2.7%)	(−1.6%)	(0.0%)
T.G.V.	Without PTMD	0.168	0.052	1.98	0.007
	With PTMD	0.163	0.048	1.93	0.007
		(3.0%)	(7.7%)	(2.5%)	(0.0%)
Design requirements		$\leqslant 1.875$ (L/1600)	$\leqslant 0.35$	$\leqslant 5.5$	$\leqslant 0.05$

Number in bracket '( )': reduction percentage.

Table 5
Maximal responses of trains and bridge B2 with and without PTMD

Train type	PTMD condition	Maximal vertical displacement at midspan (cm)	Maximal vertical acceleration at midspan (g)	Maximal rotation at right end (10^{-4} radian)	Maximal vertical acceleration at bogie (g)
I.C.E.	Without PTMD	0.255	0.045	2.02	0.006
	With PTMD	0.247	0.041	2.05	0.006
		(3.1%)	(8.9%)	(−1.5%)	(0.0%)
S.K.S.	Without PTMD	0.227	0.052	1.78	0.012
	With PTMD	0.189	0.034	1.50	0.008
		(16.7%)	(34.6%)	(15.7%)	(33.3%)
T.G.V.	Without PTMD	0.362	0.095	2.97	0.017
	With PTMD	0.281	0.055	2.32	0.011
		(22.4%)	(42.1%)	(21.9%)	(32.3%)
Design requirements		$\leqslant 1.905$ (L/2100)	$\leqslant 0.35$	$\leqslant 3.8$	$\leqslant 0.05$

Number in bracket '( )': reduction percentage.

Compared with bridge B1, the PTMD is shown to be more effective in reducing the dynamic responses of bridge B2 since the resonant train speeds are all below the design train speed. The four peak response curves under trains with speeds ranging from 0 to 350 km/h for bridge B2 are illustrated in Figs. 11–14. These figures prove that the resonant responses occur near the resonant train speeds listed in Table 2. Meanwhile, the resonant responses excited by the T.G.V. train are more apparent than those by other trains. This is due to the fact that the bridge arrangement for the T.G.V. train is more regular. The PTMD is more effective in reducing the maximal dynamic responses excited by the T.G.V. train. As shown in Table 5, the reductions are about 25% and 40% for maximal displacement and acceleration respectively. The time histories of vertical displacement and vertical acceleration of bridge B2, and the maximal vertical acceleration of T.G.V. train with a speed of 240 km/h, are illustrated in Figs. 15–17. It is obvious that the peak and overall responses are all reduced. The time history of the PTMD stroke is also plotted in Fig. 18. It is seen that the

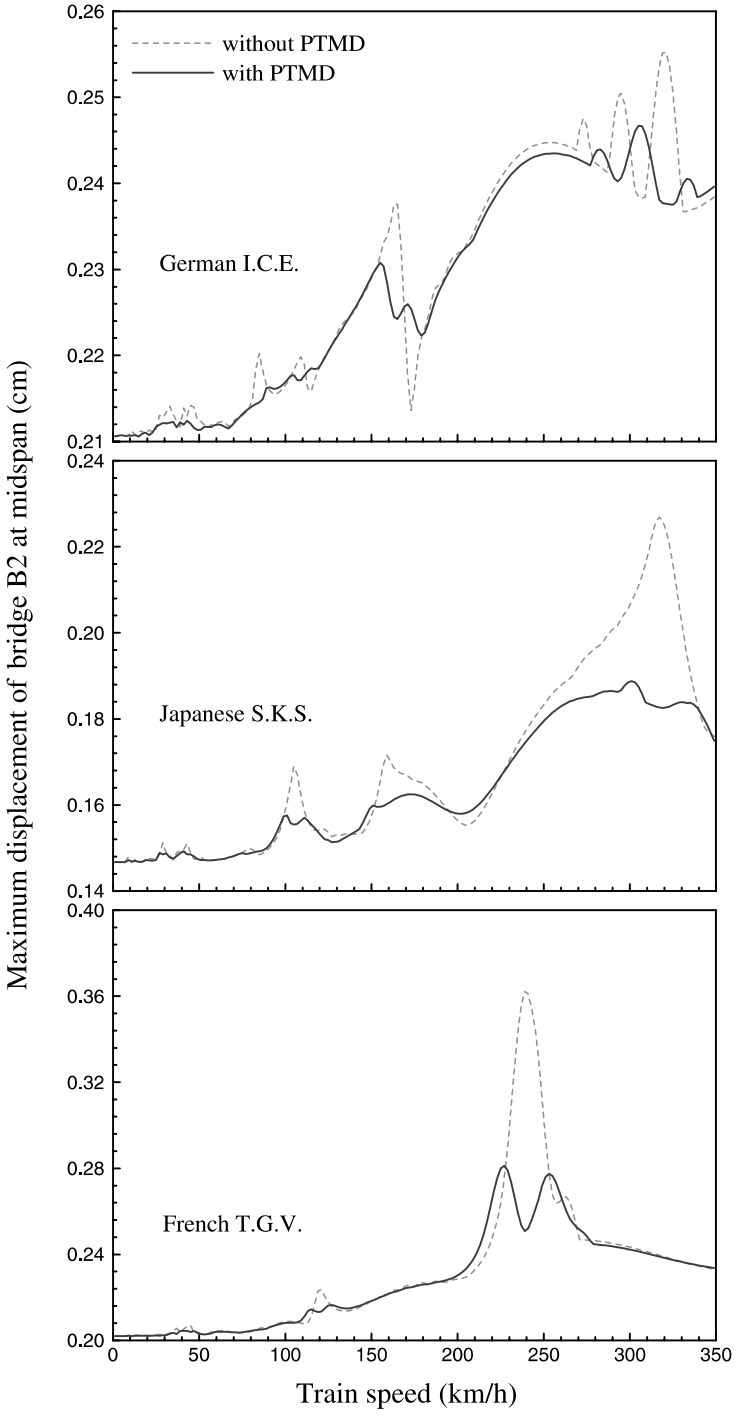

Fig. 11. Maximal displacements of bridge B2 with and without PTMD at various train speeds.

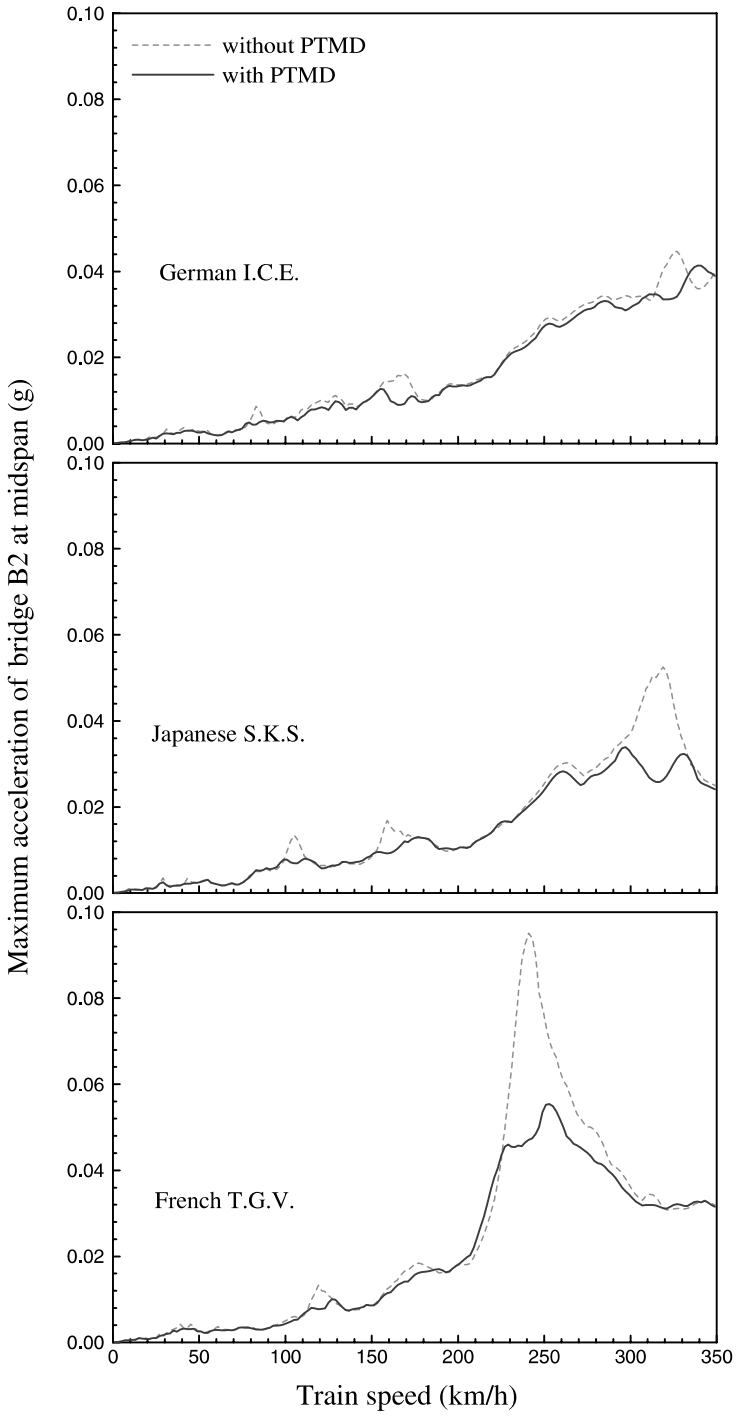

Fig. 12. Maximal accelerations of bridge B2 with and without PTMD at various train speeds.

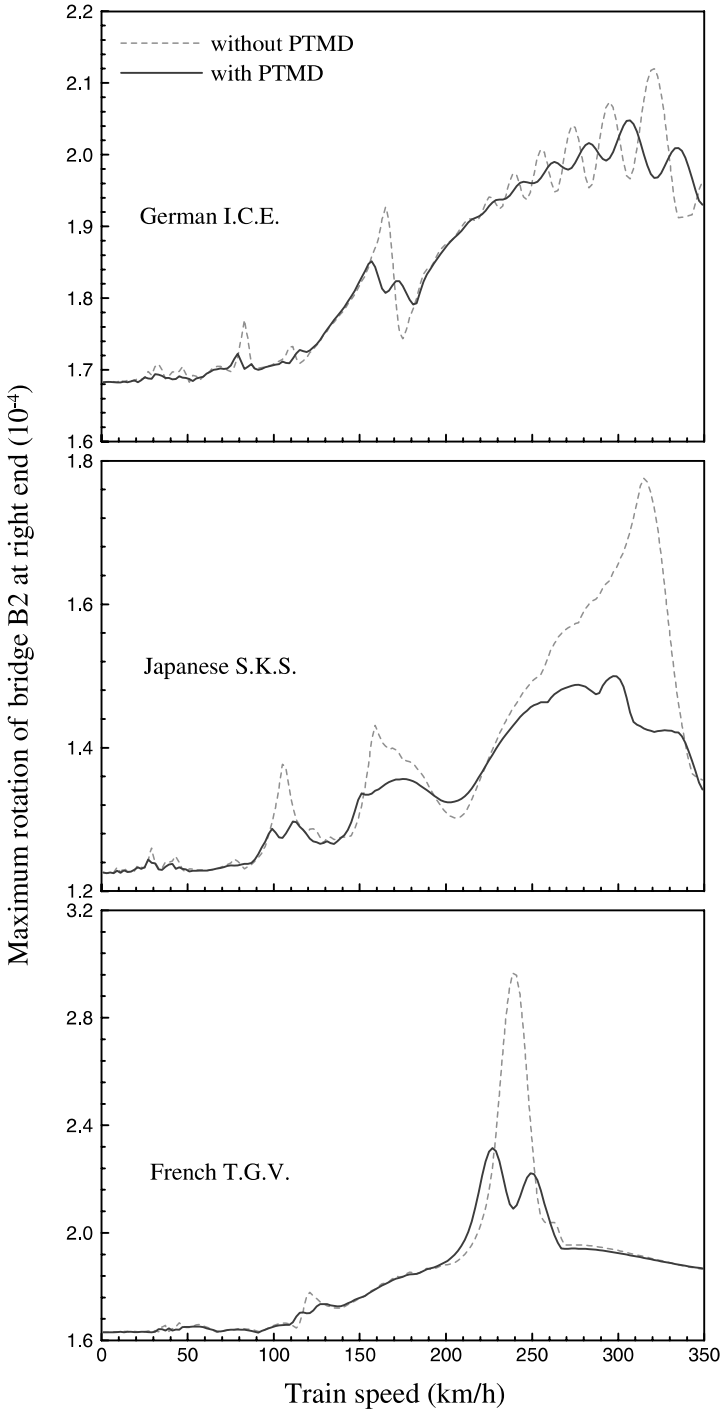

Fig. 13. Maximal rotations of bridge B2 with and without PTMD at various train speeds.

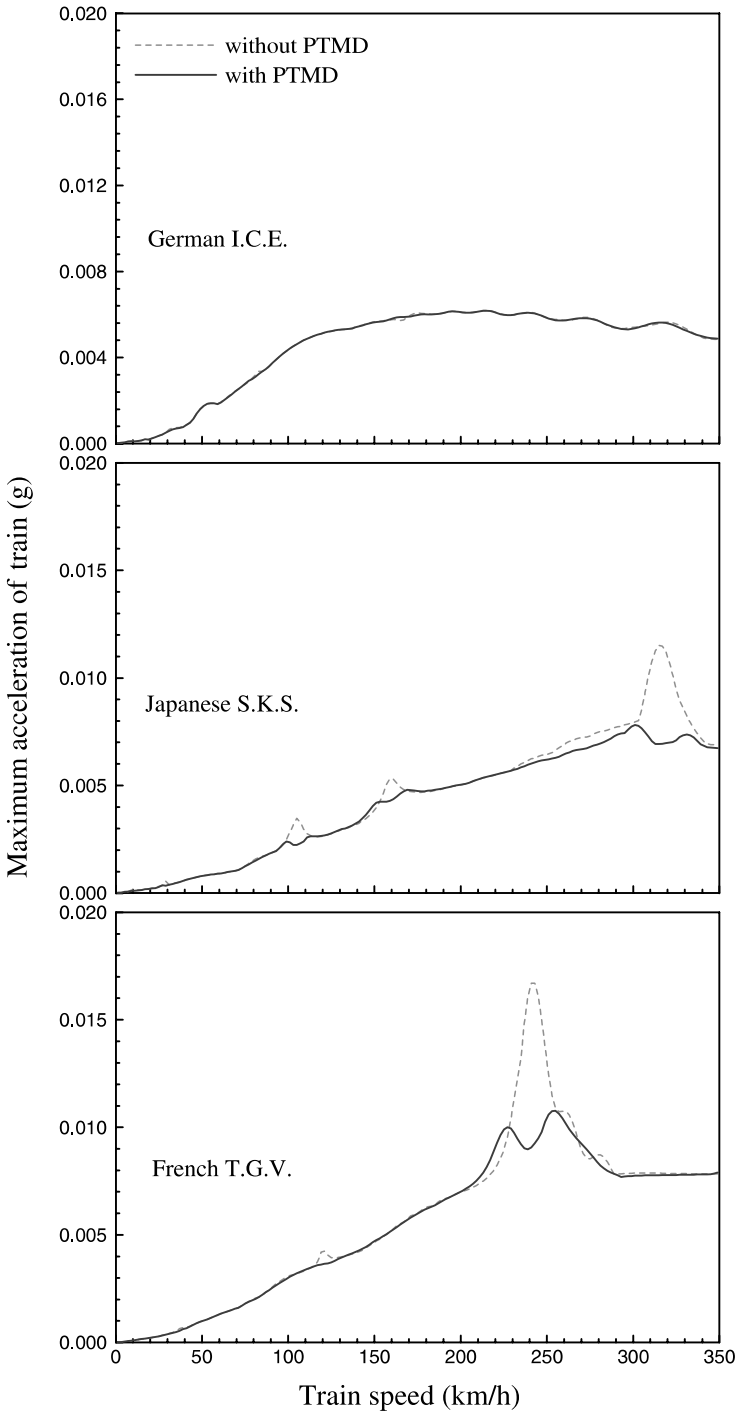

Fig. 14. Maximal accelerations of trains passing over bridge B2 with and without PTMD at various train speeds.

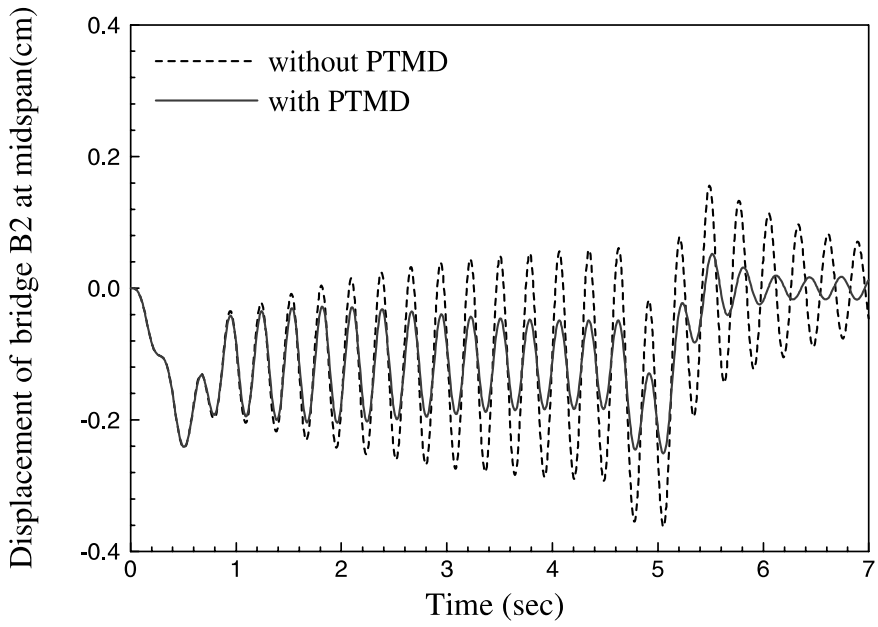

Fig. 15. Time history of the displacement of bridge B2 at the midspan under a T.G.V. train with constant speed of 240 km/h.

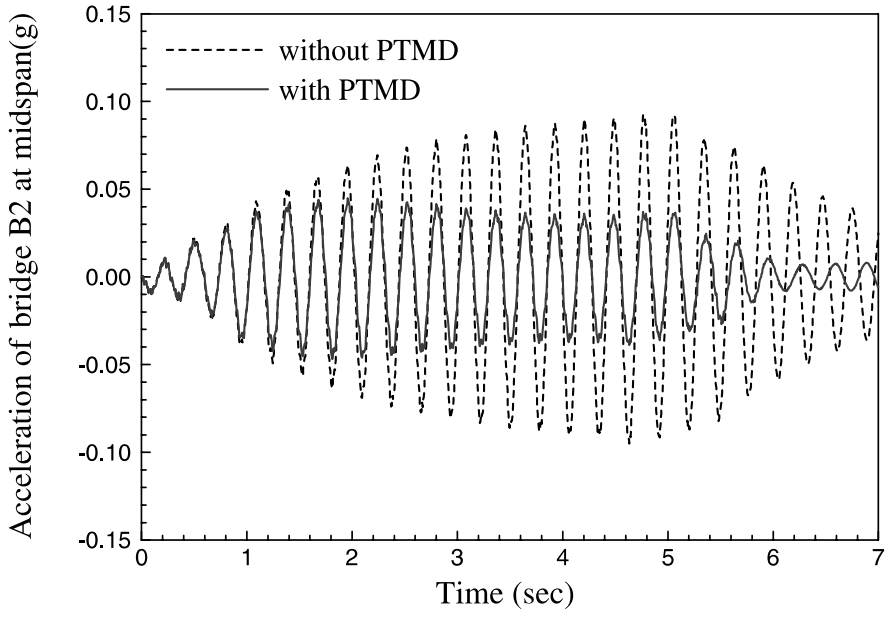

Fig. 16. Time history of acceleration of bridge B2 at the midspan under a T.G.V. train with constant speed of 240 km/h.

peak response is only 0.81 cm, much smaller than the inner depth of box girder. There is enough space for the installation and movement of PTMD.

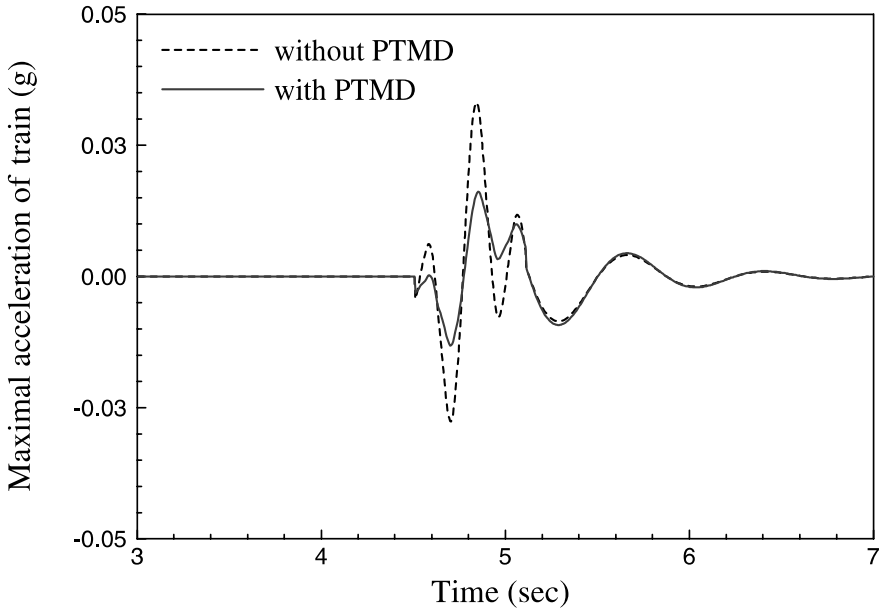

Fig. 17. Time history of maximal acceleration of a T.G.V. train with constant speed of 240 km/h.

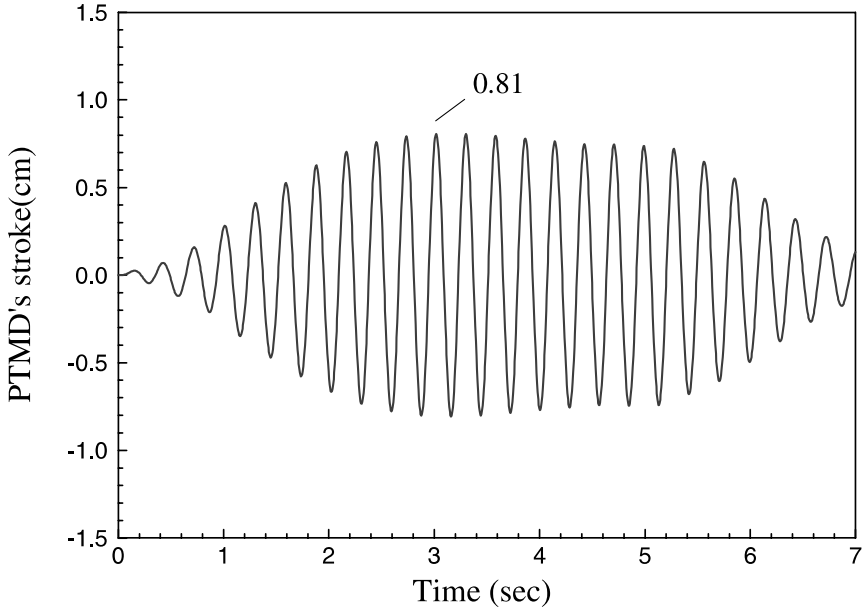

Fig. 18. Time history of PTMD's stroke for bridge B2 under a T.G.V. train with constant speed of 240 km/h.

5.2. PTMD detuning effect

The vibration suppression is achieved through tuning PTMD frequency to the vicinity of the controlled structure frequency. As stated previously, knowledge of the controlled primary structure is required in

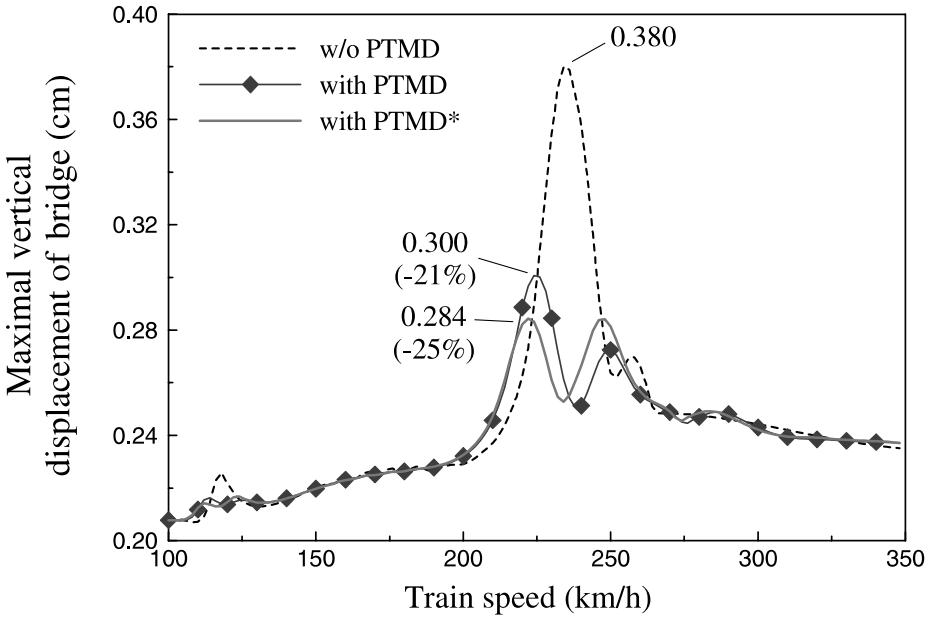

Fig. 19. Maximal vertical displacement of bridge B2 without and with two types of PTMDs (PTMD*: considering the vehicle model effect).

order to accurately calculate the optimal PTMD parameters. From previous studies, it is generally recognized that the structural natural frequency estimation error will significantly affect the PTMD design as well as its control effectiveness. This is called the detuning effect because the PTMD does not tune to the right frequency. In addition to the PTMD structural property estimation and fabrication errors, the time-variant characteristics of the combined system may also lead to the PTMD detuning effect. Thus, various dynamic interactions between the bridge and train, resulting from various vehicle models, will affect the PTMD control effectiveness. Since the PTMD is a linear system, examining the influence of such time-variant phenomena on the PTMD control effectiveness will ensure its reliability and applicability.

To investigate the problem described above, a study for bridge B2 subjected to the T.G.V. train simulated as moving mass model is performed. Fig. 19 shows the maximal vertical displacement of the bridge without and with two types of PTMDs under the train with speeds ranging from 100 to 350 km/h. The symbolized line is the bridge with the PTMD designed based on the original natural frequency of the bridge. It can be seen that two local peaks of the curves are not balanced, which is due to the PTMD detuning effect. The solid line is the same case, but considering the train model effect. The PTMD* shown in Fig. 19 is designed based on the average natural frequency of the bridge–train system, as illustrated in Figs. 3 and 4. Obviously, the PTMD* is more effective in reducing the transient response. The bridge maximal displacement reduction increases from 21% to 25%. However, this variation is relatively small. The influence of the interaction effect between the bridge and train on the PTMD control effectiveness is not significant.

6. Conclusions

A PTMD is a useful vibration control device that dissipates the structural vibration energy when the external excitation is resonant with the structure. For wind and earthquake loads, the frequency content is

wide-band and usually covers the structural dominant frequencies. Therefore, the PTMD has good control performance. For a high-speed railway train passing over a bridge with constant speed, its induced excitation frequency content has narrow bandwidth and could be far away from the bridge's natural frequencies. Thus, a PTMD has good control efficiency only when the train travels at resonant speeds.

The study of the theoretical and numerical simulation results in previous sections indicates that the following conclusions may be drawn:

(1) When natural frequencies of the bridge are multiples of the impact frequency of a train, the resonant effect will occur, even though the train is traveling at moderate speeds (less than 200 km/h).
(2) If the maximum dynamic responses of the bridge and train are dominated by the resonant response within the design train speed, the PTMD has good vibration control performance. The numerical verifications results for a moderately long bridge (bridge B2) show that the PTMD can suppress the vertical displacements, vertical accelerations, and end rotations of the bridge, and the vertical train accelerations. Among them, the maximum vertical acceleration of the bridge can be reduced up to about 40% for only 0.5% PTMD mass ratio. In addition, the PTMD stroke is small so that it can be installed inside the inner HSR box girder.
(3) The interaction between the bridge and train which leads to the PTMD detuning effect will affect the PTMD control effectiveness. A precise train model must be considered in calculating the accurate PTMD parameters. However, the influence of the interaction effect on the PTMD performance is not significant.

Acknowledgements

This work was supported by National Science Council of the Republic of China under grant NSC 86-2221-E-005-004. This support is greatly appreciated. The authors would like to thank the reviewers for their constructive comments that improved the quality of the paper.

References

Abdel-Ghaffar, A.M., Rubin, I.I., 1982. Suspension bridge response to multiple support excitations. Journal of Engineering Mechanics Division, ASCE 108, 419–434.

Akin, J.E., Mofid, M., 1989. Numerical solution for response of beams with moving mass. Journal of Structural Engineering, ASCE 115 (1), 120–131.

Boonyapinyo, V., Yamada, H., Miyata, T., 1994. Wind-induced nonlinear lateral-torsional buckling of cable-stayed bridges. Journal of Structural Engineering, ASCE 120 (2), 486–506.

Bryja, D., Sniady, P., 1988. Random vibration of a suspension bridge due to highway traffic. Journal of Sound and Vibration 125 (2), 379–387.

Chatterjee, P.K., Datta, T.K., Surana, C.S., 1994. Vibration of suspension bridges under vehicular movement. Journal of Structural Engineering, ASCE 120 (3), 681–703.

Chen, Y.H., Li, C.Y., 2000. Dynamic response of elevated high-speed railway. Journal of Bridge Engineering, ASCE 5 (2), 124–130.

Den Hartog, J.P., 1956. Mechanical Vibrations, fourth ed. McGraw-Hill, New York.

Dumanoglu, A.A., Severn, R.T., 1990. Stochastic response of suspension bridges to earthquake forces. Earthquake Engineering and Structural Dynamics 19, 133–152.

Frahm, H., 1911. Device for damping vibrations of bodies. US patent 989-958.

Frýba, L., 1996. Dynamics of Railway Bridges, second ed. Thomas Telford, London.

Frýba, L., 2001. A rough assessment of railway bridges for high speed trains. Engineering Structure 23 (5), 548–556.

Green, M.F., Cebon, D., Cole, D.J., 1995. Effects of vehicle suspension design on dynamic of highway bridges. Journal of Structural Engineering, ASCE 121 (2), 272–282.

Hayashikawa, T., Watanabe, N., 1981. Dynamic behavior of continuous beams with moving loads. Journal of Engineering Mechanics Division, ASCE 107, 229–246.

Hayashikawa, T., Watanabe, N., 1982. Suspension bridge response to moving loads. Journal of Engineering Mechanics Division, ASCE 108, 1051–1066.

Huang, D.Z., Wang, T.L., 1992. Impact analysis of cable-stayed bridges. Computers and Structures 43 (5), 897–908.

Huang, D.Z., Wang, T.L., Shahawy, M., 1998. Vibration of horizontally curved box girder bridges due to vehicles. Computers and Structures 68, 513–528.

Huang, D.Z., Wang, T.L., 1998. Vibration of highway steel bridges with longitudinal grades. Computers and Structures 69, 235–245.

Humar, J.L., Kashif, A.H., 1995. Dynamic response analysis of slab-type bridges. Journal of Structural Engineering, ASCE 121 (1), 48–62.

Hutton, S.G., Cheung, Y.K., 1979. Dynamic response of single span highway bridges. Earthquake Engineering and Structural Dynamics 7, 543–553.

Inbanathan, M.J., Wieland, M., 1987. Bridge vibrations due to vehicle movement over rough surfaces. Journal of Structural Engineering, ASCE 113 (9), 1994–2008.

Kajikawa, Y., Okino, M., Uto, S., Matsuura, Y., Iseki, J., 1989. Control of traffic vibration on urban viaduct with tuned mass dampers. Journal of Structural Engineering, JSCE 35A, 585–595.

Klasztorny, M., Langer, J., 1990. Dynamic response of single-span beam bridges to a series of moving loads. Earthquake Engineering and Structural Dynamics 19, 1107–1124.

Kou, J.W., De Wolf, J.T., 1997. Vibrational behavior of continuous span highway bridge-influencing variables. Journal of Structural Engineering, ASCE 123 (3), 333–344.

Kwon, H.C., Kim, M.C., Lee, I.W., 1998. Vibration control of bridges under moving loads. Computers and Structures 66 (4), 473–480.

Lin, C.C., Hu, C.M., Wang, J.F., Hu, R.Y., 1994. Vibration control effectiveness of passive tuned mass dampers. Journal of the Chinese Institute of Engineers 17 (3), 367–376.

Lin, T.Y., Taiwan, 1993. Vibrations of Elevated Bridge Structures Caused by High-Speed Train Loadings of Taiwan High-Speed Rail Project (Final Report). Taiwan High Speed Rail Bureau, Ministry of Transportation and Communications, R.O.C.

Veletsos, A.S., Huang, T., 1970. Analysis of dynamic response of highway bridges. Journal of Engineering Mechanics Division, ASCE 96, 593–620.

Vellozzi, J., 1967. Vibration of suspension bridges under moving loads. Journal of Structural Engineering, ASCE 93 (4), 123–138.

Wang, T.L., Shahawy, M., Huang, D.Z., 1992. Impact in highway prestressed concrete bridges. Computers and Structures 44 (3), 525–534.

Wilson, J.F., Barbas, S.T., 1980. Response of continuous elasticity supported beam guideways to transit loads. Journal of Dynamic System, Measurement, Control, ASME 102, 247–254.

Yang, Y.B., Yau, J.D., Hsu, L.C., 1997. Vibration of simple beams due to train movement at high speeds. Engineering Structure 19 (11), 936–944.